NASA TECHNICAL MEMORANDUM

NASA TM X- 68246

NASA TM X- 68246

ENGINE-OVER-THE-WING NOISE RESEARCH

by Meyer Reshotko, Jack H. Goodykoontz, and Robert G. Dorsch
Lewis Research Center
Cleveland, Ohio 44135

TECHNICAL PAPER proposed for presentation at
Sixth Fluid and Plasma Dynamics Conference sponsored
by the American Institute of Aeronautics and Astronautics
Palm Springs, California, July 16-18, 1973

ENGINE-OVER-THE-WING NOISE RESEARCH

Meyer Reshotko*, Jack H. Goodykoontz*, and Robert G. Dorsch*

National Aeronautics and Space Administration
Lewis Research Center
Cleveland, Ohio

Abstract

Acoustic measurements for large model engine-over-the-wing (EOW) research configurations having both conventional and powered lift applications were taken for flap positions typical of takeoff and approach and at locations simulating flyover and sideline. The results indicate that the noise is shielded by the wing and redirected above it, making the EOW concept a prime contender for quiet aircraft. The large-scale noise data are in agreement with earlier small-model results. Below the wing, the EOW configuration is about 10 PNdB quieter than the engine-under-the-wing externally-blown-flap for powered lift, and up to 10 dB quieter than the nozzle alone at high frequencies for conventional lift applications.

Introduction

E-7429

During the past decade airplane propulsion systems have become louder, sprawling cities have moved closer to their airports and the general awareness of noise has made the public particularly sensitive to aircraft noise. This has led to threatened airport closings, airport curfews, and stringent noise regulations, which in some cases cannot be met by current state-of-the-art techniques. Also, in order to provide high speed transportation between city centers, powered lift aircraft such as STOL (Short Takeoff and Landing) and RTOL (Reduced Takeoff and Landing) vehicles using shorter runways have been proposed. This is a difficult engineering task because the lift augmentation device necessary for powered lift generates and redirects noise, while the total noise levels of the aircraft must be compatible with the local community. A possible solution to the CTOL (Conventional Takeoff and Landing), STOL, and RTOL noise problems is to place the engine over the wing. With such a configuration, the wing shields the ground from some of the engine noise and redirects it above the aircraft.

Engine-over-the-wing (EOW) noise and static lift tests have been made with small models.[1-6] These tests included various shaped nozzles with both powered and conventional lift applications, and a variety of attachment devices all making use of the Coanda effect[7] which causes the exhaust jet to attach itself to the upper surface of the wing and flaps. One of the combinations which achieved good noise shielding by the wing and good flow turning in the powered lift mode was the circular nozzle with deflector. This configuration, with and without a flow deflector, was scaled up to a large model from which the acoustic scaling laws can be checked and from which more accurate noise predictions can be made for full-sized aircraft.

A large model experimental study, similar to the one made for the engine-under-the-wing externally blown flap,[8] was conducted in order to measure noise level and directivity patterns for powered and conventional lift EOW configurations. Air supplied to a convergent nozzle placed over a wing section simulated the engine-over-the-wing configuration for the CTOL case (fig. 1(a)). The nozzle exit diameter was 13 in. and the wing chord was 7 ft. For powered lift, a nozzle-flow deflector was used to obtain flow attachment to the upper surface of the wing and flaps for lift augmentation. In the experiment, the flap slots were covered (fig. 1(b)). The jet exhaust velocities ranged from 550 to 1000 ft/sec. Acoustic measurements were taken with flap angles corresponding to takeoff and approach and at various azimuthal angles corresponding to flyover and sideline.

The large model EOW noise data, having both powered and conventional lift applications, are reported in this paper. The results are also compared to recently-taken small model and TF-34 full scale engine data for scaling effects. For the powered lift case, the large EOW model data are compared to data for an under-the-wing externally-blown-flap configuration of the same model size.

Apparatus, Procedure, and Acoustic Analysis

Model description. - The configuration and dimensions of typical EOW test models having both conventional and powered lift applications are shown in Fig. 2. For conventional lift applications (fig. 2(a)), the model consisted of a partial span wing with a double-slotted flap and a convergent circular nozzle. The wing section had a chord length of 82 in., with the flaps retracted, and a span of 9 ft. The flaps could be placed in any one of three settings: (1) leading flap 30° from the wing chord line, trailing flap 60°; (2) leading flap 10°, trailing flap 20°; and (3) zero angle (retracted). The wing was mounted on a stand with the spanwise direction vertical.

Tests were conducted for all flap settings with the slots between the flaps either open or covered with thin gauge sheet metal. The sheet metal extended over the entire upper surface of the wing in the spanwise direction, and from the trailing edge of the trailing flap to a location directly under the nozzle in the chordwise direction.

A convergent nozzle was used in all tests. The nozzle had a 13-in. diameter exit located 13 in. downstream of the wing leading edge, and a center line located 12-1/4 in. above the upper surface of the wing. The nozzle axis was located 12-3/4 ft above grade.

For powered lift applications (STOL), a deflector plate was mounted above the nozzle as shown in Fig. 2(b). The deflector plate was 19-1/2 in. wide and centered over the nozzle with a deflection angle of 30° for all flap positions. The remainder of the wing model was the same as that used for the CTOL tests. Photographs of typical large EOW models

*Aerospace Research Engineers, Jet Acoustics Branch, V/STOL and Noise Division.

used in the tests are presented in Fig. 1. The conventional lift configuration is shown in Fig. 1(a) with the wing slots open and flaps in the 30°-60° setting. Figure 1(b) shows the model in the powered lift configuration with the deflector plate, slots covered, and wing flaps in the 10°-20° setting.

Nozzle air supply system. - A schematic drawing of the airflow system is shown in Fig. 3. Dry air (45° to 80° F) was supplied to a 16-in. diameter gate shut off valve through an underground pipe line from the Center's air supply system (150 psi max). A metering orifice was located upstream of the gate valve in a straight section of the underground pipe line. A 10 in. diameter butterfly valve was used to control the flow to the nozzle.

A muffler system installed in the line downstream of the flow control valve attentuated internal noise caused primarily by the flow control valve. The muffler system consisted of perforated plates and dissipative type mufflers. The perforated plates were located immediately downstream of the flow control valve (40 percent open area) and at the entrance and exit of the first dissipative muffler (20 percent open area). Both dissipative mufflers were sections of pipe that housed crossed splitter plates oriented at right angles to one another so that the flow was divided into four channels. The internal surfaces of the muffler pipes and the surfaces of the splitter plates were covered with an acoustic absorbent material. The second dissipative muffler was located downstream of the last 45° elbow in the airflow line to take advantage of the reflections caused by turning the flow. In addition, the flow system was wrapped externally with fiberglass and leaded vinyl to impede direct radiation of internal noise through the pipe wall.

Two screens were placed in the air line downstream of the last muffler to improve the flow distribution to the nozzle. Total pressure and temperature were measured directly upstream of the nozzle. Nozzle exhaust velocities were calucated from the isentropic equations.

Test procedures. - Far field noise data were taken over a range of nozzle pressure ratios for each model configuration. The pressure ratios (nozzle total pressure divided by atmospheric pressure) ranged from 1.2 to 1.8. Nozzle total temperature varied between 45° and 80° F. The calculated nozzle exhaust velocities based on the nozzle pressure ratios and total temperatures ranged between 550 and 1000 ft/sec.

Acoustic analysis. - Noise measurements using 1/2-in. condenser microphones were taken at various locations simulating flyover and sideline (fig. 4). Seventeen microphones were appropriately placed on a 50 ft radius circle in a horizontal plane perpendicular to the vertically mounted wing for the flyover-mode noise measurements. The center of the microphone circle was located on the nozzle axis 23 in. downstream of the nozzle exit. The microphones and nozzle axis were 12-3/4 ft above the hard surfaced ground.

Sideline noise measurements were made in the spanwise direction in a plane perpendicular to the flyover or horizontal plane. This sideline or vertical plane intersects the flyover plane at an angle from the nozzle inlet where the flyover noise is a maximum for the particular configuration being tested (fig. 4). The sideline noise data were taken by suspending a microphone from the boom of a mobile crane. The microphone was 50 ft from the nozzle axis in all cases, and at the angular locations shown in Fig. 4. The sideline angles indicated are those made with the vertically mounted wing and include 0°, 27°, 45°, 60°, and 90° (which is in the horizontal plane).

The noise data were analyzed by a 1/3-octave band spectrum analyzer which determined sound pressure level spectra referenced to 0.0002 microbar. Three noise data samples were taken at each microphone location for each pressure ratio. An atmospheric loss correction was applied to the average of the three samples to give lossless sound pressure level data at 50 ft. From these sound pressure level spectra the overall sound pressure levels were calculated at each microphone location. Except as indicated no ground reflection corrections were made to the noise data.

Results and Discussion

The large model acoustic results associated with the engine-over-the-wing concept are separated into two main categories: powered lift, for STOL and RTOL applications; and conventional lift for CTOL applications. Each category has sections on flyover noise, sideline noise and comparisons with small model data. In addition, the powered lift category has comparisons with an engine-under-the-wing model.

Powered Lift Configurations (STOL, RTOL Applications)

A deflector was used to obtain nozzle exhaust flow attachment to the upper surface of the wing and flaps for powered lift simulation. Flow turning angles of 30° and 60° were achieved for flap positions typical of takeoff and approach respectively.[5,6] Previously reported noise measurements[2,6] were taken with open and closed flap slots, but the noise levels were considerably less with the slots closed. Therefore, all the noise data presented in this category were taken with the flap slots covered.

Flyover noise. - A most basic form of acoustic data is the sound pressure level (SPL) spectrum. With these data, the overall sound pressure level (OASPL) and the perceived noise level (PNL) for any given configuration can be obtained. One-third octave band SPL spectra for the EOW configuration are shown in Fig. 5 for a microphone distance of 50 ft and a nozzle exhaust velocity range of 680 to 945 ft/sec. Data are presented for a two flap system with flap positions of 10°-20° and 30°-60°, which are typical for takeoff and approach respectively. The spectra shown are for the maximum under-the-wing noise which occurs at 80° and 100° from the nozzle inlet, for the respective flap positions of 30°-60° and 10°-20°. Although no corrections have been made for ground reflections, the frequencies at which the first few reinforcements and cancellations take place are indicated by the R and C locations. The peak SPL values occur at the low frequencies (about 200 Hz) and drop off by more than 25 dB at 20 000 Hz. Although the peak SPL values are the same for both flap positions, the data at 10°-20° are 2 to 4 dB quieter at the

higher frequencies than at 30°-60°.

The EOW noise radiation patterns for both flap positions are shown in Fig. 6. The configuration, exhaust velocities and microphone distance are the same as for the previously described spectra. The radiation pattern is fairly uniform in the region in front of and under the wing, in contrast to what happens above the wing. In the third quadrant, which is above the wing, the OASPL values are up to 10 dB higher than under the wing. It is this redirection of the noise that makes the engine-over-the-wing concept attractive.

The effect of shielding and redirection of noise by the wing for the EOW concept with powered lift is shown in Fig. 7. The noise was measured at 50 ft and the microphone angular locations correspond to the maximum under-the-wing or flyover noise for their respective flap positions. The nozzle exhaust velocities of 765 and 680 ft/sec were assumed to be representative of takeoff and approach respectively, for some powered lift systems. The three spectra in each of Figs. 7(a) and 7(b) are corrected for ground reflections and represent the nozzle alone, nozzle with deflector and nozzle with deflector and wing. By adding the deflector, which is necessary to obtain powered lift in this configuration, there is a large increase in noise with respect to the nozzle alone at the middle and high frequencies. The addition of the wing, which completes the EOW model, caused a sharp decrease in high frequency noise and shifted the peak SPL from 500 Hz to about 200 Hz. The wing and flaps act as a good shield for high frequency noise, but generate low frequency noise as the flow passes over the trailing edge of the last flap. Since the low frequency trailing-edge noise is about the same above and below the wing, this large decrease in high frequency noise causes the large reductions in OASPL below the wing as illustrated in Fig. 6. At an angle of 80° (fig. 7(b)) the nozzle alone SPL values at 10 000 Hz are 2 dB greater than the EOW configuration, while at 100° (fig. 7(a)) they are 4 dB greater. This occurs because the high frequency noise for the configuration peaks at the indicated angles while for the nozzle alone it peaks at 120°.[9] Data similar to that in Fig. 7(a) at 120° shows that, at high frequency, the nozzle alone would be about 9 dB greater than that for the nozzle, deflector and wing configuration.

The effect of exhaust velocity on the flyover noise for the EOW model with powered lift is shown in Fig. 8. Acoustic data for a third flap position, retracted flaps, are included. The OASPL values in Fig. 8(a) are for a common microphone angle of 90° at 50 ft. The data for all three flap positions follow the sixth power velocity relationship very well. This is in agreement with previously reported flap noise data.[3] Maximum flyover PNL values calculated to 500 ft are shown in Fig. 8(b). The 10°-20° flap position is the quietest of the three, with 30°-60° being one to two PNdB louder, and the retracted flaps being about one PNdB above that. These values are proportional to the shielding of noise by the wing and flap system. The 10°-20° flap position shields the most, while the retracted flap position shields the least.

Sideline noise. - In addition to the flyover measurements, noise data were also taken at various sideline locations. In Fig. 9 there is a comparison of flyover and sideline noise for the EOW model with powered lift. All the sideline acoustic data were taken in the vertical plane passing through the 100° microphone location (fig. 4). The microphone angles in this plane are referenced to the vertically mounted wing. Zero degrees represents the wing tip sideline location, 90° represents flyover, and the 27° location is sometimes used as a guideline for powered lift aircraft. If an observer is 500 ft to the side of the runway and an aircraft is 250 ft above the runway, the angle between the aircraft wing and observer is 27°. Spectral values of flyover and sideline noise are shown in Fig. 9(a) for a microphone distance of 50 ft and a nozzle exhaust velocity of 760 ft/sec. At low frequencies the flyover mode has the greatest noise, while at the middle and high frequencies the 0° sideline mode is loudest. This occurs because at low frequencies the trailing edge noise is most evident in the flyover mode, and at high frequencies there is no shielding at 0° sideline. On a perceived noise level basis, with velocity as the abscissa (fig. 9(b)), the acoustic values at 0° sideline and at flyover are almost the same. This occurs because the PNL calculation weights the high frequency SPLs more than the low frequency SPLs. The sideline noise measurements reach a minimum at 27°. Data were also taken at 45° and 60°, but the results fall below the maximum and above the minimum and are therefore not shown.

Comparison with small model data. - This large model experiment was based on one of many small model engine over the wing tests conducted at the Lewis Research Center.[1-7] The 13-in. nozzle and 7-ft wing-chord were scaled up by a factor of 6.5 from a 2-in. diameter nozzle and 13-in. wing-chord. The small model noise data were taken at a 10 ft radius.

In order to compare 1/3-octave spectral data, it is necessary to scale the magnitude of the sound pressure level and frequency. The frequency is scaled using the Strouhal relationship (St) between frequency (f), velocity (V), and nozzle diameter (D) where

$$St = \frac{f_{\text{small model}}\, D_{\text{s.m.}}}{V_{\text{s.m.}}} = \frac{f_{\text{large model}}\, D_{\text{l.m.}}}{V_{\text{l.m.}}}$$

The validity of using Strouhal scaling for flap noise was established by Dorsch[8] for the under-the-wing externally-blown-flap and is assumed to apply for the EOW as well. The magnitude of the small model SIL or OASPL values can be scaled up to large model results by using the Lighthill relationship for area increase and the inverse square law for change in microphone radius (R). This results in the following scale factor which must be added to the small model data in order to get large model results at a 50 ft radius

$$10 \log \left[\left(\frac{D_{\text{l.m.}}}{D_{\text{s.m.}}} \right)^2 \times \left(\frac{R_{\text{s.m.}}}{R_{\text{l.m.}}} \right)^2 \right] =$$

$$10 \log \left[\left(\frac{13}{2} \right)^2 \times \left(\frac{10}{50} \right)^2 \right] = 2.3 \text{ dB}$$

In Fig. 10 a comparison is made of large model data with scaled up small model data at the same velocity, for the EOW configuration with powered lift using the previously discussed scaling techniques. For both models the flaps were at 10°-20°, and the nozzle exhaust velocity was 945 ft/sec. The spectral data (fig. 10(a)), at 100° from the inlet, show good agreement between the two models. The small discrepencies that do exist at the lower frequencies can be attributed to ground reflections. In Fig. 10(b) the noise radiation patterns of the two models are compared, with the magnitude of the small model OASPL scaled up by 2.3 dB. Under the wing, between 60° and 140° from the inlet, the data scale within one dB. Above the wing, between 180° and 360° from the inlet, the large model data are about 5 dB greater than the scaled up small model data. This indicates that the shielded flap noise scales quite well, but the reflected noise does not.

By carrying the concept of Strouhal scaling one step further and normalizing the data with respect to velocity, the Strouhal correlation for large model data is obtained as shown in Fig. 11. The 1/3-octave SPL data obtained at a microphone angle of 100° and a flap setting of 10°-20° for the large model were first corrected for ground reflections and then converted to Normalized SPL Spectral Density (SPL-OASPL + 10 log V/D Δf) and plotted with respect to the Strouhal number (fD/V). The data points shown are for nozzle exhaust velocities between 550 to 1000 ft/sec. The curve shown was obtained from a fit to a similar set of small model data. Figure 11 shows that the Strouhal relation correlates the large model data very well over the velocity range and that there is a very good agreement between the large and small model data. The only significant discrepancy between the results of the two models is in the high frequency slope. Above a Strouhal number of two, the large model values of normalized SPL spectral density decrease at a somewhat lower rate with frequency than those for the small model.

Comparisons with TF-34 data. - An acoustic program was conducted under the direction of the Lewis Research Center using a quieted TF-34 engine. The TF-34 was tested in the EOW configuration with internal noise suppression and a mixed exhaust exiting from a 37-in. diameter conical nozzle. In addition to the engine, the configuration consisted of a flow deflector and a wing and flap system. The trailing flap was at 40° with respect to the wing chord, which is the takeoff position for this configuration.

In Fig. 12 large model data are compared with scaled up small model data and scaled down TF-34 data for the EOW configuration with powered lift. The data were taken at 100° from the nozzle inlet with the flaps in the takeoff position and an exhaust velocity of 765 ft/sec. In order to account for differences in microphone distance, and a small variation in exhaust velocity for the TF-34 engine, the sound pressure levels are normalized with respect to their corresponding values of OASIL. The respective frequencies are determined by Strouhal scaling. The data from all three models are in good agreement with only small differences at low frequencies due to ground reflections.

The results of Figs. 10-12 show that there is very good agreement between the data of this study and the previous small model results. In addition, the results also show that there is good agreement between the data for the large model (with simulated exhaust) and the TF-34 configuration which is representative of a full size EOW system employing an actual engine.

Comparison with engine-under-the-wing model. - A comparison was made between the EOW model and an engine-under-the-wing externally-blown-flap model similar to the one reported in Ref. 8. The engine-under-the-wing model used the same 13-in. nozzle and wing section and had triple flaps with the same trailing flap angles of 20° and 60° as the EOW model. The position of the nozzle relative to the wing and flaps was selected to produce, the authors' believe, similar lift augmentation as the EOW model. A spectral comparison of the engine-over-the-wing and under-the-wing configurations with powered lift at angles producing maximum flyover noise are shown in Fig. 13(a) and 13(b) for the 20° and 60° trailing flap positions respectively. The nozzle-over-the-wing SPL values peak at a lower frequency than those for the nozzle-under-the-wing. Also, above 200 Hz, the over-the-wing model is about 10 dB quieter because of wing shielding.

The effects of wing shielding and noise redirection can best be seen by the radiation patterns shown in Fig. 14. Here, the perceived noise levels at 500 ft are compared for both models at both trailing flap angles. The EOW system is much quieter below the model, where it is most important, and slightly noiser above. At 90°, which would be directly under an aircraft, the EOW system is about 10 PNdB quieter than the EBF under-the-wing system. The dependence of noise on nozzle exhaust velocity is shown for both the over and under-the-wing systems in Fig. 15. The perceived noise levels at 500 ft are shown for microphone angles giving maximum noise at flyover. At both trailing flap angles, the EOW system is about 10 PNdB quieter in the velocity range shown. In each part of Fig. 15 the curves are parallel, indicating that both systems have the same velocity dependence.

In summarizing the comparison between the two systems, the EOW is quieter by about 10 dB above 200 Hz and 10 PNdB quieter at angles under the model for exhaust velocities between 550 to 1000 ft/sec for the scale of the models tested.

Conventional Lift Configurations (CTOL Applications)

All the noise data presented in this category were taken with the flap slots open and the flow deflector removed (figs. 1(a) and 2(a)). The flow circulation through the open slots is desirable for lift, while the noise values were about the same whether the slots were open or closed. Although the nozzle exhaust was not attached to the upper surface of the flaps, there was still some flow interaction with the trailing edge of the wing.

Flyover noise. - One-third octave band sound pressure level (SPL) spectra for the EOW configuration are shown in Fig. 16 for a microphone distance of 50 ft and a nozzle exhaust velocity range of 675 to 985 ft/sec. Data are presented for a two flap system with flap positions of 10°-20° and 30°-60°, which are typical for takeoff and approach

respectively. The spectra shown are for the maximum under-the-wing noise which occurs at 120° from the nozzle inlet for both flap positions. Although no corrections have been made for ground reflections, the frequencies at which the first few reinforcements and cancellations take place are indicated. The peak SPL values occur at the low frequencies (between 200 and 400 Hz) and drop off by 16 to 22 dB at 20 000 Hz. Although the peak SPL values are the same at both flap positions, the 10°-20° case is about 2 dB quieter at the higher frequencies than the 30°-60° case.

The EOW noise radiation patterns for both flap positions are shown in Fig. 17. The configuration, exhaust velocities and microphone distance are the same as in Fig. 16. The radiation patterns are fairly uniform between 20° and 120° and reach a maximum at 200°. At 200°, the OASPL values are greater than those at the flyover maximum of 120° by 5-8 dB for the 10°-20° flap position and 4-7 dB for the 30°-60° flap position.

The effect of shielding and redirection of noise by the wing for the EOW concept with conventional lift applications is shown in Fig. 18. The noise was measured at 50 ft and 120° from the nozzle inlet, the angle of the maximum flyover noise for both flap positions. The nozzle exhaust velocities of 985 and 885 ft/sec were assumed to be representative of takeoff and approach respectively for advanced conventional lift aircraft. The two spectra in each of Figs. 18(a) and 18(b) represent the nozzle alone, and the nozzle-over-the-wing configuration. The addition of the wing, which completes the EOW model, causes up to a 10 dB decrease in high frequency noise, while just slightly increasing the low frequency noise. The wing and flaps again act as a good shield for high frequency noise, and because the jet flow is unattached to the flaps, there is little low frequency trailing edge noise.

The effect of flap position on the maximum flyover noise spectra for the EOW model with conventional lift is shown in Fig. 19. Acoustic results for a third flap position, retracted flaps, are also included. The data are for a nozzle exhaust velocity of 830 ft/sec, at a microphone distance of 50 ft at 120° from the inlet. At frequencies above 2000 Hz the 10°-20° flap position is the quietest, with the 30°-60° position being one to two dB louder, and the retracted flaps being a few dB above that. Again, like the powered lift case, these values are proportional to the amount of noise shielded by the wing and flap system. The 10°-20° flap position offers the most shielding, while the retracted flaps offers the least.

The effect of velocity on the flyover noise for the EOW model with conventional lift is shown in Fig. 20. The OASPL values in Fig. 20(a) are for a microphone angle of 120° at 50 ft. The data for all three flap positions follow the eighth power velocity relationship. Maximum PNL values calculated to 500 ft are shown in Fig. 20(b). The 10°-20° flap position is the quietest of the three, with the 30°-60° position being one PNdB louder, and the retracted flaps being one more PNdB above that. These noise levels at different flap positions have the same relationship to each other as their corresponding spectra above 2000 Hz (fig. 19). This happens because the frequencies above 2000 Hz make a large contribution to the perceived noise level.

Sideline noise. - In addition to the flyover measurements, noise data were also taken at various sideline locations. In Fig. 21 there is a comparison of flyover and sideline noise for the EOW model with conventional lift. All the acoustic data were taken in the vertical plane passing through the 120° microphone location (fig. 4). The microphone angles in this plane are referenced to the vertically mounted wing. Flyover is at 90°, and the wing tip sideline location is at 0°. Spectral values of flyover and sideline noise are shown in Fig. 21(a) for a microphone distance of 50 ft and a nozzle exhaust velocity of 965 ft/sec. Below 2000 Hz the noise is greatest at flyover because although the flow is unattached to the upper surface of the flaps there is still some interaction between the jet and the trailing edge of the wing. Above 2000 Hz the wing tip sideline noise is the greatest because there is no shielding at that location. These data are also presented with OASPL as a function of velocity in Fig. 21(b).

Comparison with small model data. - In Fig. 22 a comparison of large model data is made with scaled up small model data at the same velocity, for the EOW configuration with conventional lift using the scaling techniques discussed in the powered lift scaling section. For both models the flaps were at 10°-20° and the nozzle exhaust velocity was 940 ft/sec. The spectral data (fig. 22(a)), at 120° from the inlet, show good agreement between the two models. The discrepancies that do exist can be attributed to ground reflections. Similar scaling results were also obtained between small and large model data at the 30°-60° flap position. In Fig. 22(b) the noise radiation patterns of the two models are compared with the magnitude of the small model OASPL scaled up by 2.3 dB. Under the wing, between 60° and 160° from the inlet, the data scales within 2 dB. Above the wing, the large model data are up to 5 dB greater than the scaled up small model data.

The Strouhal correlation for the large model data is shown in Fig. 23 for both flap positions. The 1/3-octave SPL data obtained at a microphone angle of 120° for the large model were first corrected for ground reflections and then converted to Normalized SPL Spectral Density and plotted with respect to the Strouhal number. The data points shown are for nozzle exhaust velocities between 625 to 1000 ft/sec. The curve shown was obtained from a fit to a similar set of small model data. Figure 23 shows that the Strouhal relation correlates the large model data very well over the velocity range and that there is good agreement between the small and large model data. The only discrepancy between the results of the two models again is in the high frequency slope.

Shielding effectiveness. - The shielding effectiveness of the EOW configuration for conventional lift applications for both flap positions is shown in Fig. 24. The ordinate is the difference between the normalized SPL spectral density of the nozzle alone ($\overline{SPL}_n$) and the EOW configuration ($\overline{SPL}_c$), and the abscissa is Strouhal number. Above a Strouhal number of 0.7 the EOW configuration is quieter than the nozzle alone because of wing shielding.

Concluding Remarks

A large model experimental investigation has been conducted in order to determine the acoustic benefits of the engine-over-the-wing concept for both conventional and powered lift applications. By placing the engine over the wing, the region under the wing is acoustically shielded from the noise which is reflected away. The amount of noise shielding increases with increasing frequencies. This shielding benefit makes the EOW concept a contender for quiet aircraft. Below the wing, the EOW configuration is about 10 PNdB quieter than an engine-under-the-wing externally-blown-flap for powered lift, and up to 10 dB quieter than the nozzle alone at high frequencies for conventional lift applications.

The large model acoustic results were compared with small model and TF-34 engine data. In the region under the wing, the EOW noise data scale well for all models, while in the region above the wing where the noise is reflected, the scaling is not as good. Because of the good scaling in the region under the wing, models can be used as acoustical research tools and for preliminary acoustic predictions for full sized aircraft.

References

1. Reshotko, M., Olsen, W. A., and Dorsch, R. G., "Preliminary Noise Tests of the Engine-Over-the-Wing Concept. I. 30°-60° Flap Position," TM X-68032, 1972, NASA, Cleveland, Ohio.

2. Reshotko, M., Olsen, W. A., and Dorsch. R. G., "Preliminary Noise Tests of the Engine-Over-the-Wing Concept. II. 10°-20° Flap Position," TM X-68104, 1972, NASA, Cleveland, Ohio.

3. Dorsch, R. G., Lasagna, P. L., Maglieri, D. L., and Olsen, W. A., "Flap Noise," SP-311, 1972, NASA, Washington, D.C.

4. Dorsch, R., and Reshotko, M., "EBF Noise Tests with Engine Under-and-Over-the-Wing Configurations," SP 320, 1972, NASA, Washington, D.C.

5. von Glahn, U., Reshotko, M., and Dorsch, R., "Acoustic Results Obtained with Upper-Surface-Blowing Lift-Augmentation Systems," TM X-68159, 1972, NASA, Cleveland, Ohio.

6. Dorsch, R., Reshotko, M., and Olsen, W., "Flap Noise Measurements for STOL Configurations Using External Upper Surface Blowing," Paper 72-1203, 1972, AIAA, New York, N.Y.

7. von Glahn, U. H., "Use of the Coanda Effect for Jet Deflection and Vertical Lift with Multiple-Flat-Plate and Curved-Plate Deflection Surfaces," TN 4377, 1958, NACA, Cleveland, Ohio.

8. Dorsch, R. G., Kreim, W. J., and Olsen, W. A., "Externally-Blown-Flap Noise," Paper 72-129, 1972, AIAA, New York, N.Y.

9. Olsen, W. A., Gutierrez, O., and Dorsch, R. G., "The Effect of Nozzle Inlet Shape, Lip Thickness, and Exit Shape and Size on Subsonic Jet Noise," Paper 73-187, 1973, AIAA, New York, N.Y.

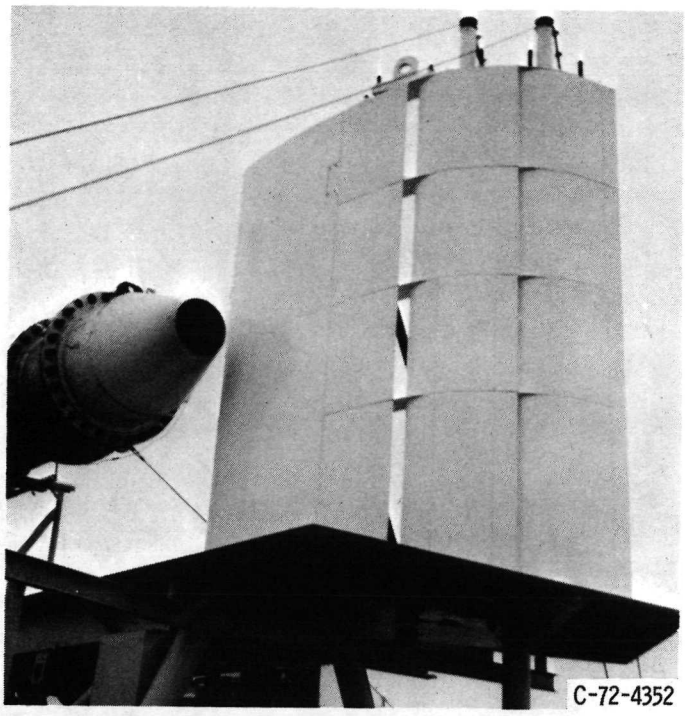

(a) CONVENTIONAL LIFT APPLICATIONS (CTOL). FLAP ANGLES, 30^{0}-60^{0} (APPROACH).

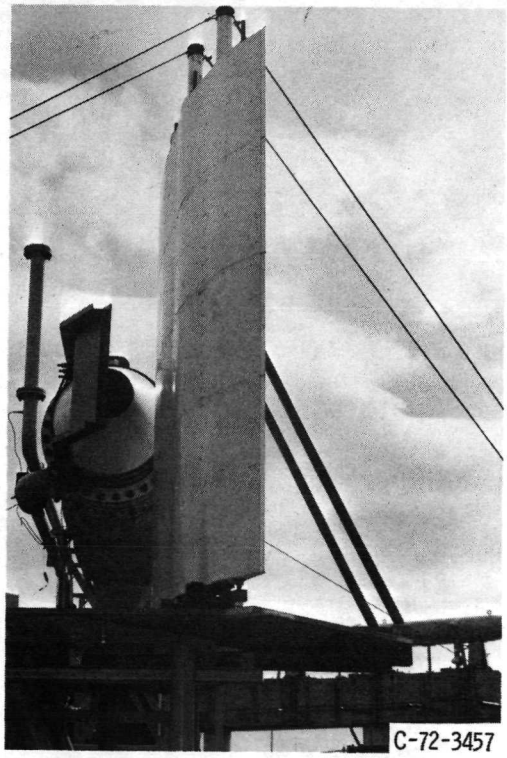

(b) POWERED LIFT APPLICATIONS (STOL, RTOL). FLAP ANGLES, 10^{0}-20^{0} (TAKEOFF).

Figure 1. - Large model engine-over-the-wing configurations. Nozzle diameter, 13 in., wing chord, 7 ft.

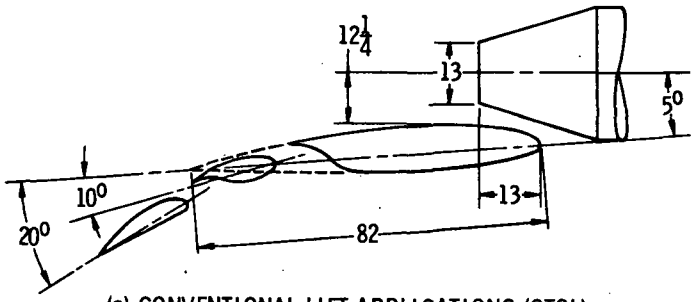

(a) CONVENTIONAL LIFT APPLICATIONS (CTOL).
FLAP ANGLES, 10°-20° (TAKEOFF).

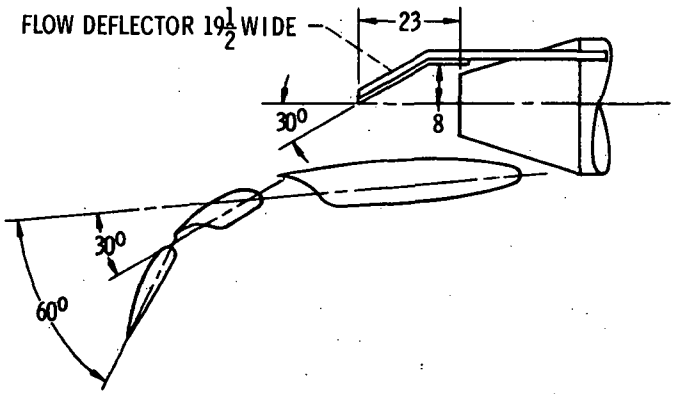

(b) POWERED LIFT APPLICATIONS (STOL, RTOL).
FLAP ANGLES, 30°-60° (APPROACH).

Figure 2. - Test configurations for the large model engine over the wing. All dimensions in inches.

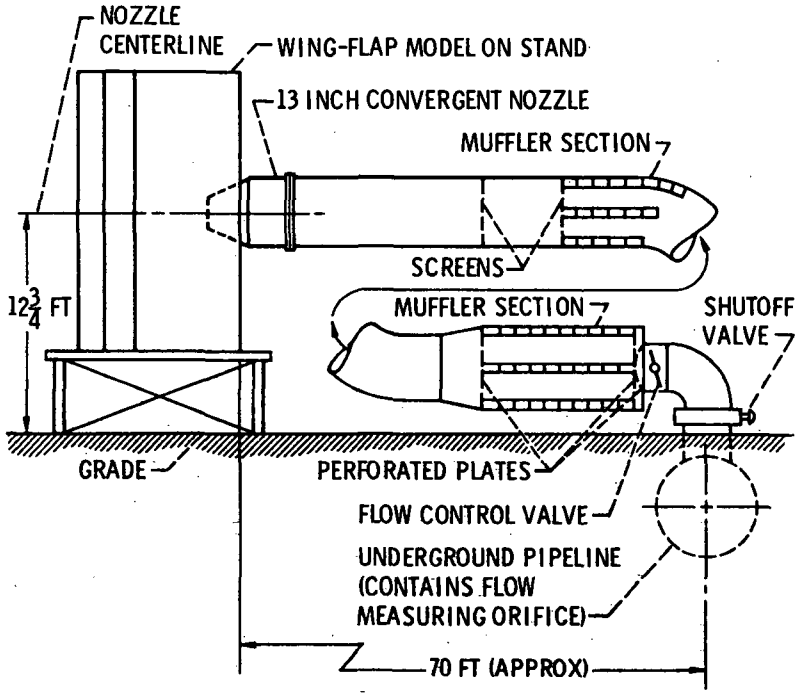

Figure 3. - Nozzle air supply system.

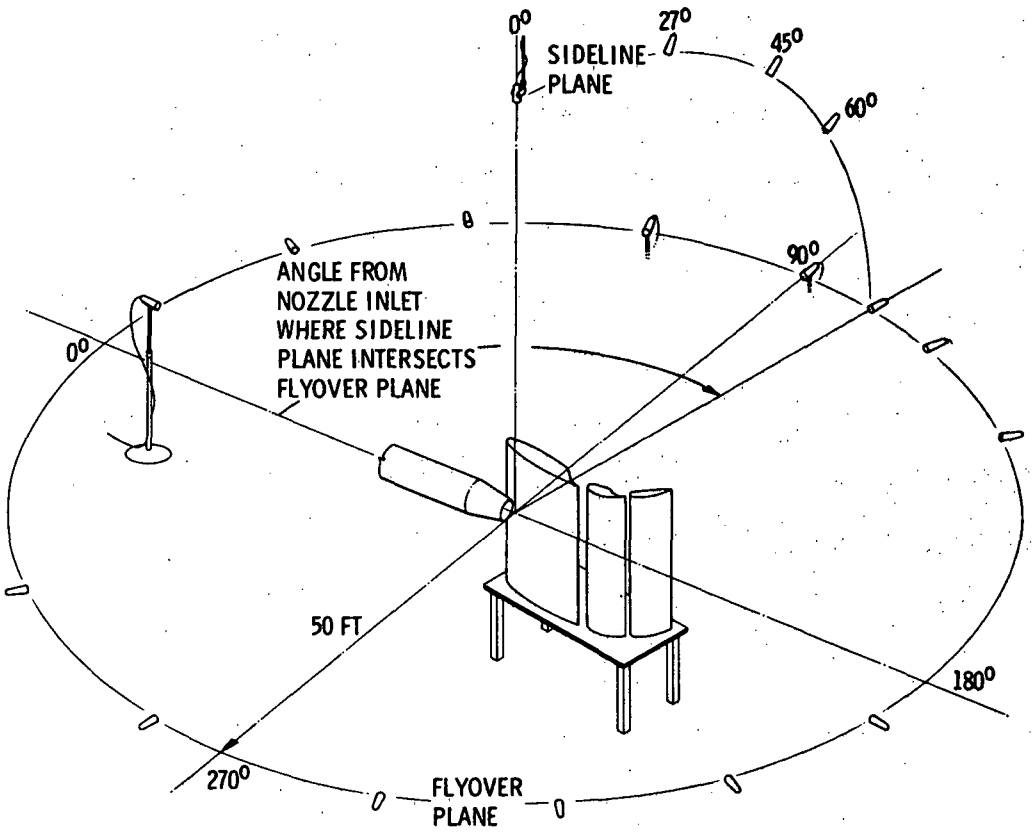

Figure 4. - Microphone layout for taking flyover and sideline mode noise data.

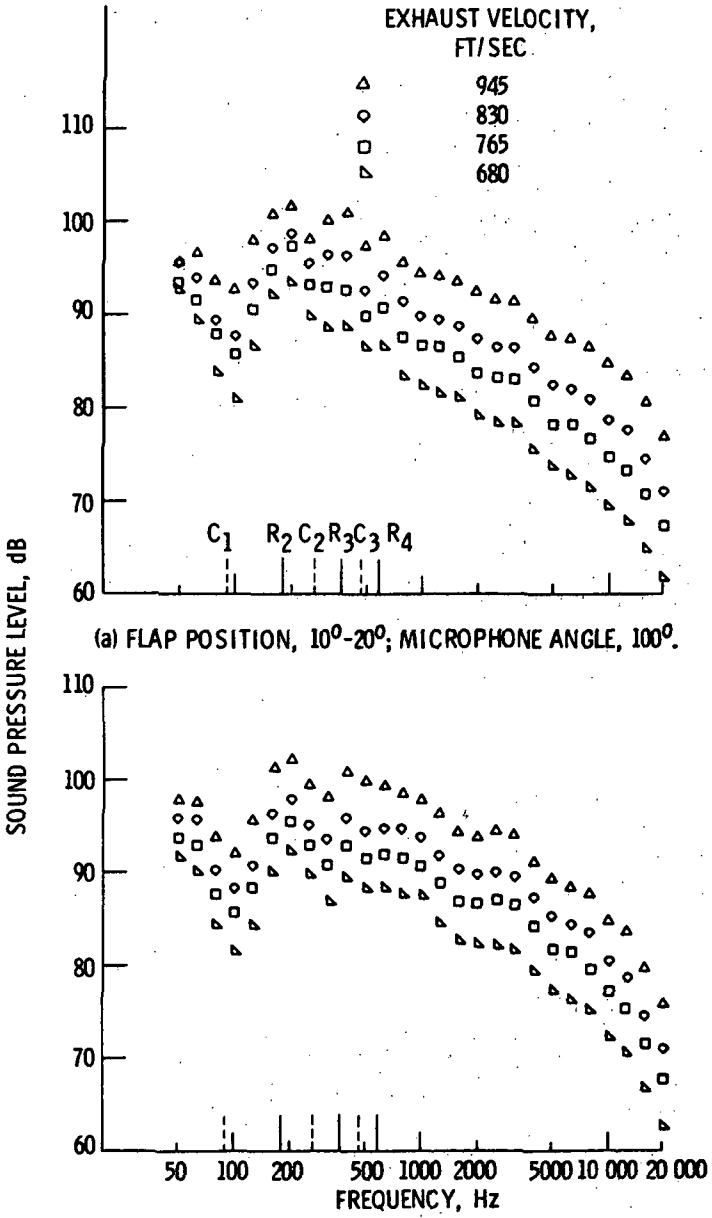

(a) FLAP POSITION, 10^0-20^0; MICROPHONE ANGLE, 100^0.

(b) FLAP POSITION, 30^0-60^0; MICROPHONE ANGLE, 80^0.

Figure 5. - EOW 1/3-octave spectra for powered lift. Microphone distance, 50 ft.

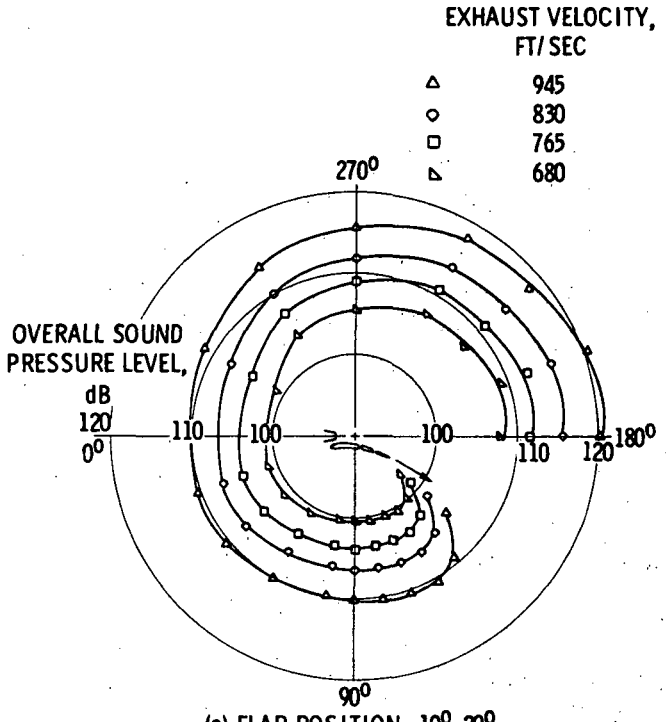

(a) FLAP POSITION, 10°-20°.

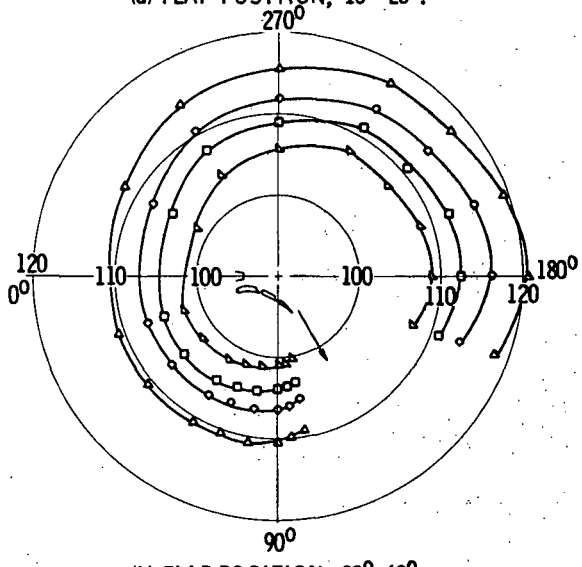

(b) FLAP POSITION, 30°-60°.

Figure 6. - EOW noise radiation patterns for powered lift. Microphone distance, 50 ft.

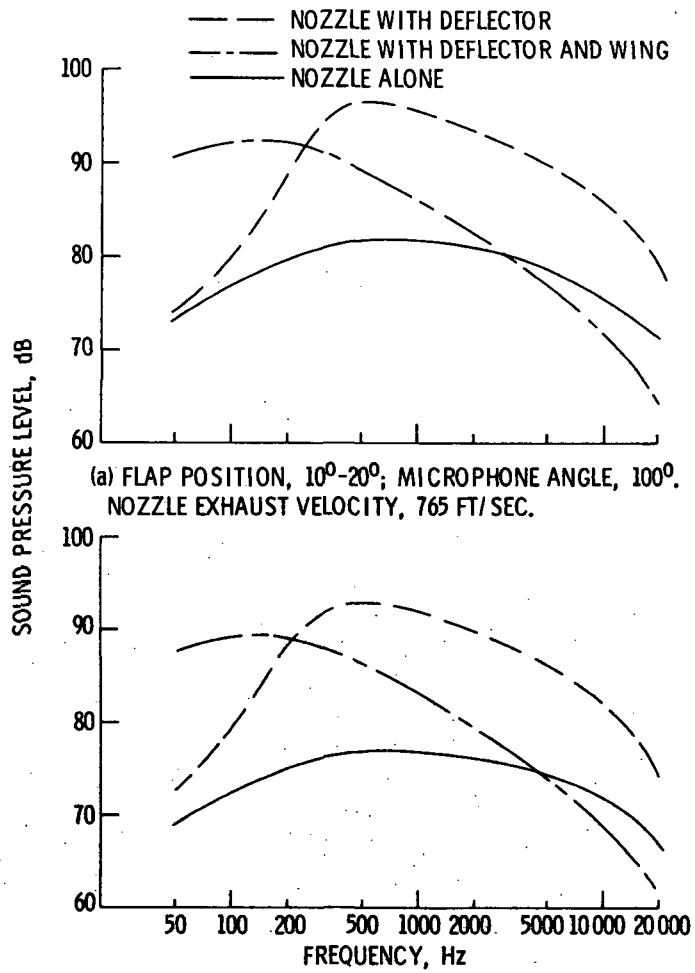

(a) FLAP POSITION, 10^0-20^0; MICROPHONE ANGLE, 100^0. NOZZLE EXHAUST VELOCITY, 765 FT/SEC.

(b) FLAP POSITION, 30^0-60^0; MICROPHONE ANGLE, 80^0. NOZZLE EXHAUST VELOCITY, 680 FT/SEC.

Figure 7. - Effect of noise shielding by the wing on the EOW configuration with powered lift. Microphone distance, 50 ft. Corrected for ground reflections.

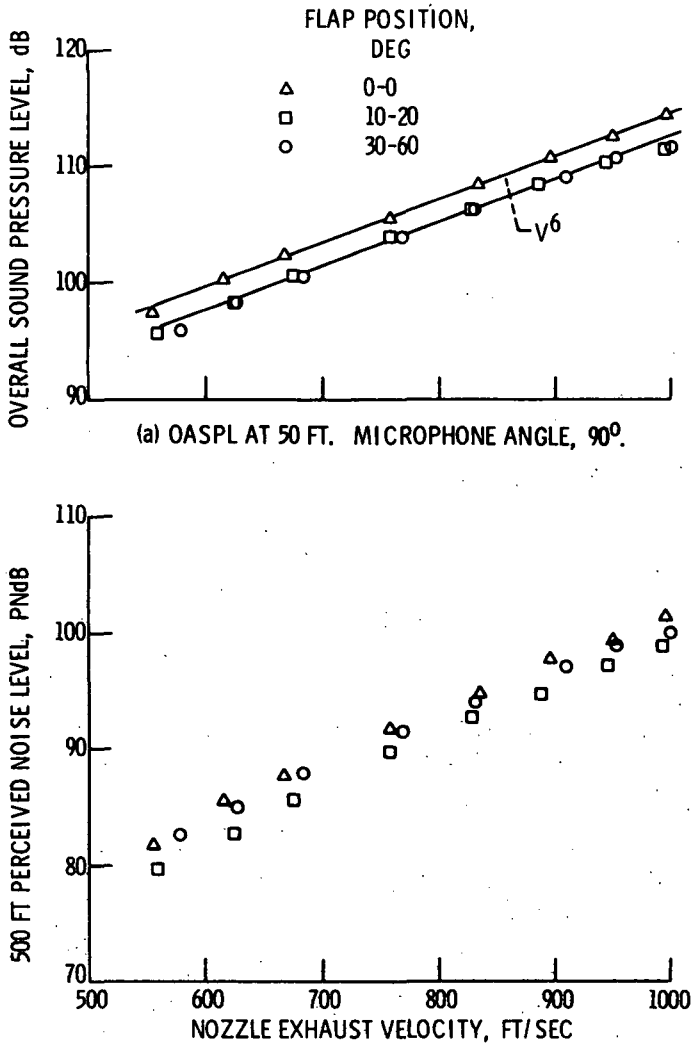

(a) OASPL AT 50 FT. MICROPHONE ANGLE, 90^0.

(b) PERCEIVED NOISE LEVEL AT 500 FT AT MICROPHONE ANGLE PRODUCING FLYOVER MAXIMUM.

Figure 8. - Effect of exhaust velocity on the flyover noise for the EOW model with powered lift.

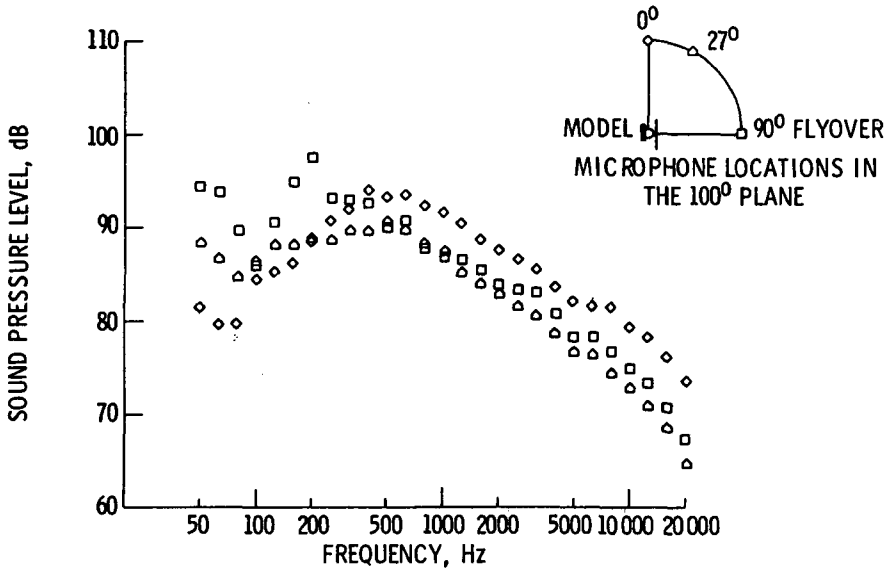

(a) 1/3-OCTAVE SPECTRA AT 50 FT. NOZZLE EXHAUST VELOCITY, 760 FT/SEC.

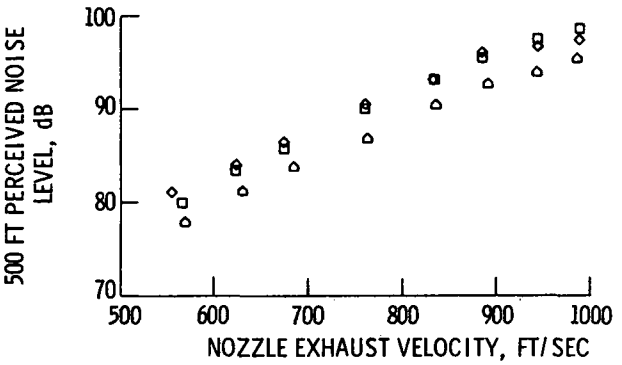

(b) PERCEIVED NOISE LEVEL AT 500 FT.

Figure 9. - Comparison of flyover and sideline noise for the EOW model with powered lift. Flap position, 10°-20°; microphones in the 100° plane.

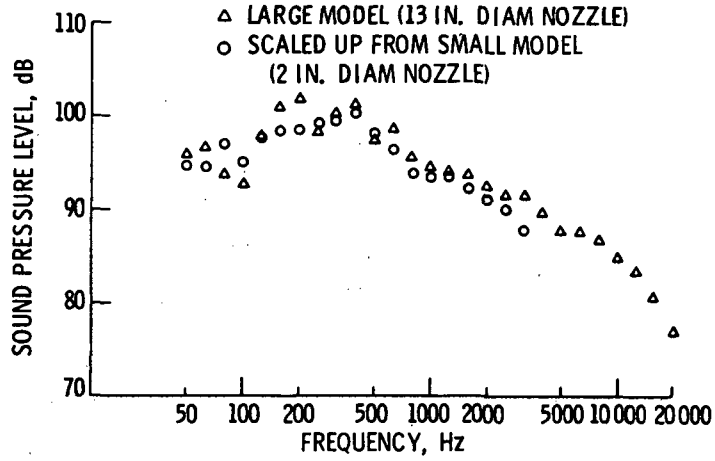

(a) 1/3-OCTAVE SPECTRA. MICROPHONE ANGLE, 100°.

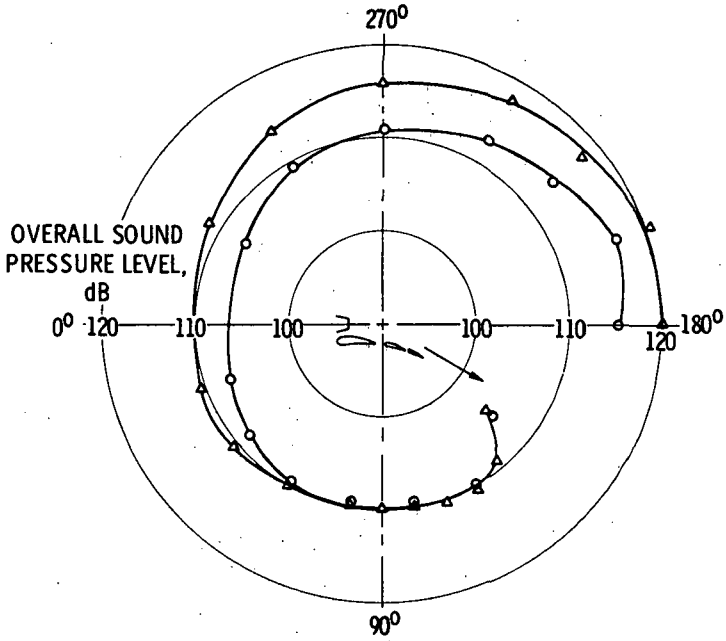

(b) NOISE RADIATION PATTERN.

Figure 10. - Comparison of large model data with scaled up small model data for the EOW configuration with powered lift. Flap position, 10°-20°; nozzle exhaust velocity, 945 ft/sec; microphone distance, 50 ft.

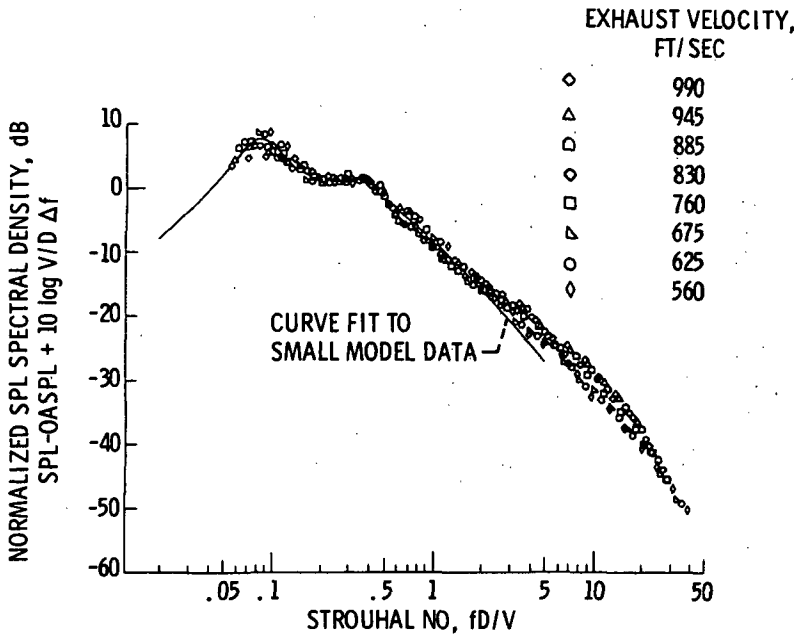

Figure 11. - A Strouhal correlation of large model data for the EOW configuration with powered lift. Flap position, 10^{0}-20^{0}; microphone angle, 100^{0}. Corrected for ground reflections.

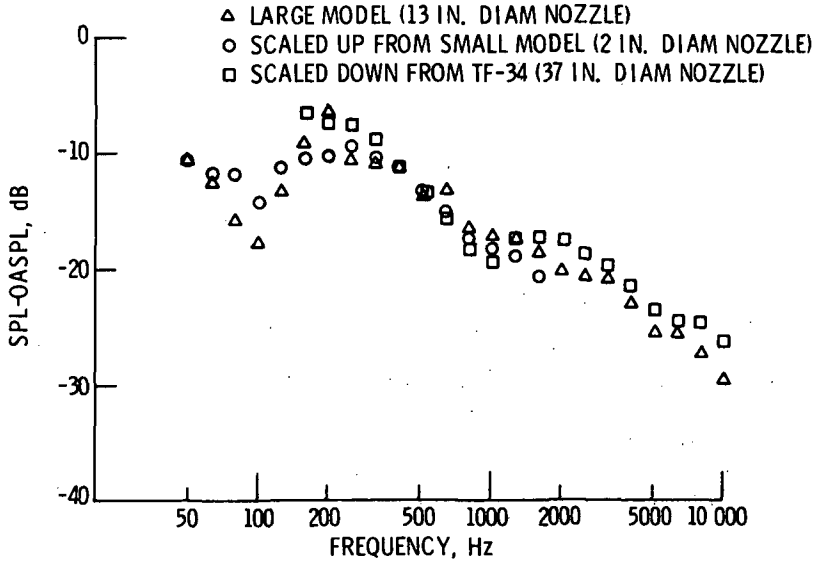

Figure 12. - Comparison of large model data with small model and TF-34 data for the EOW configuration with powered lift. Flaps in takeoff position; microphone angle, 100^{0}.

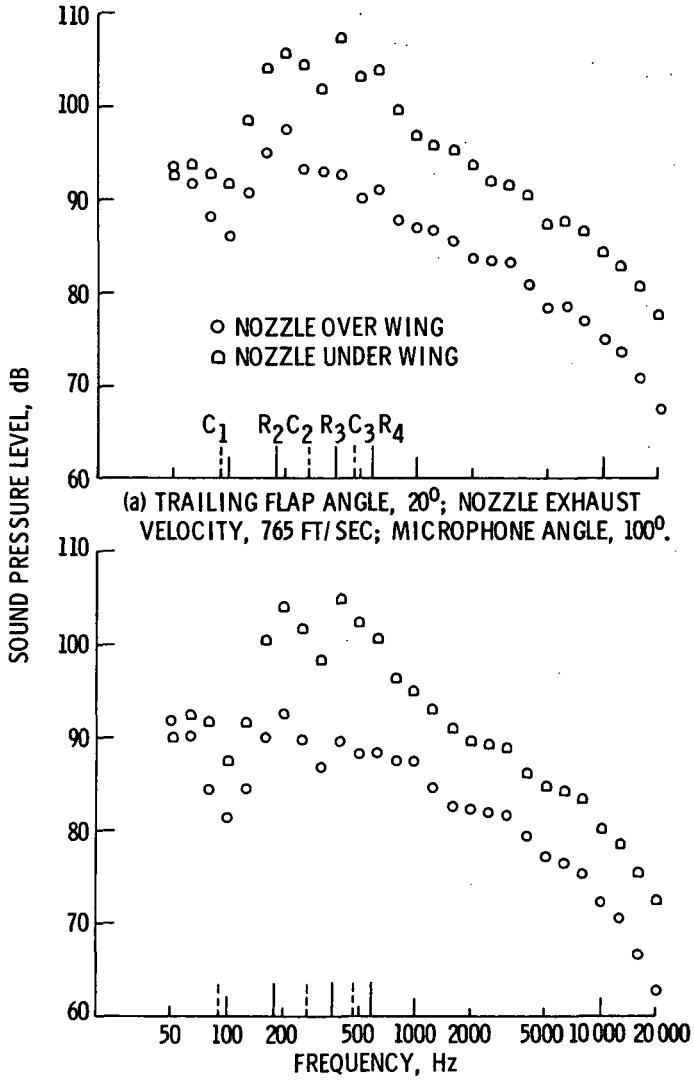

(a) TRAILING FLAP ANGLE, 20°; NOZZLE EXHAUST VELOCITY, 765 FT/SEC; MICROPHONE ANGLE, 100°.

(b) TRAILING FLAP ANGLE, 60°; NOZZLE EXHAUST VELOCITY, 680 FT/SEC; MICROPHONE ANGLE, 80°.

Figure 13. - Spectral comparison of the engine over the wing and under the wing models with powered lift. Microphone distance, 50 ft.

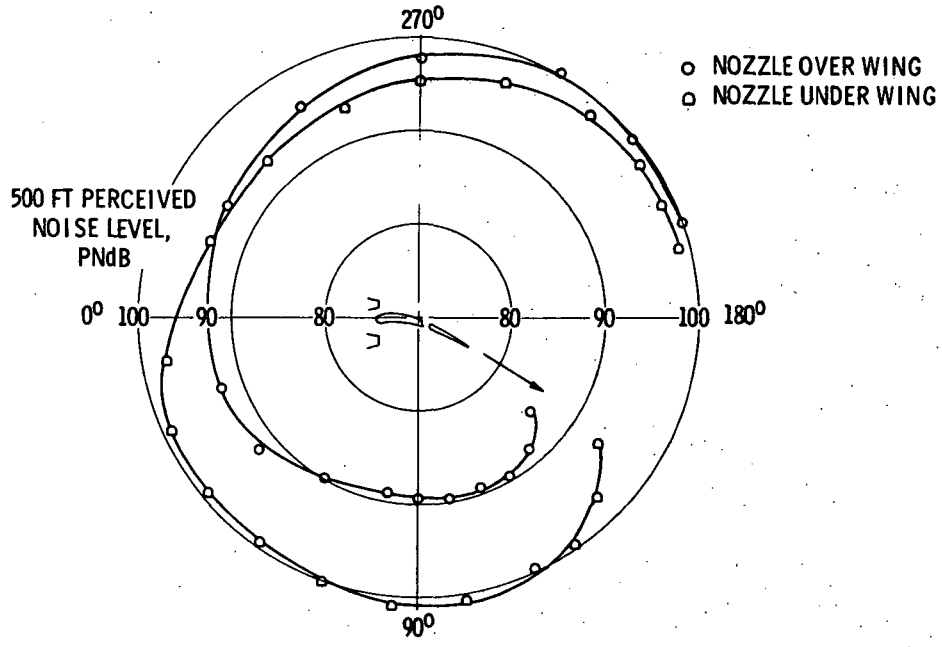

(a) TRAILING FLAP ANGLE, 20°; NOZZLE EXHAUST VELOCITY, 765 FT/SEC.

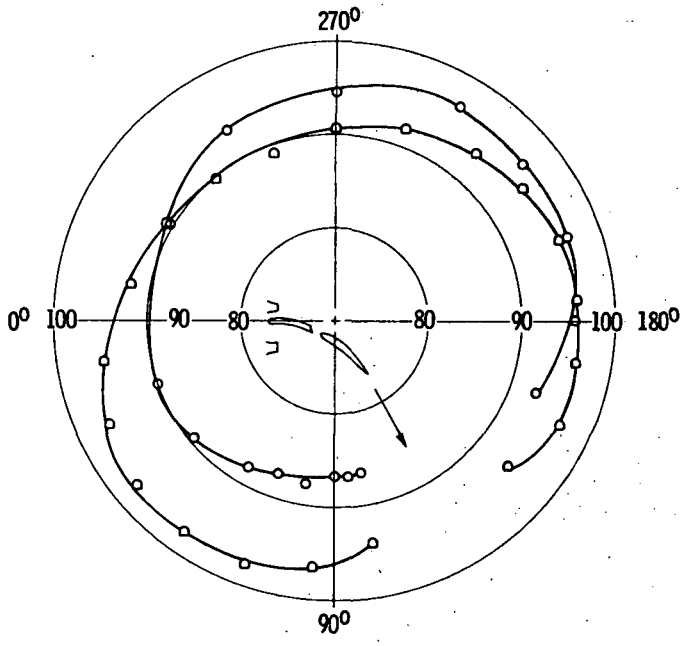

(b) TRAILING FLAP ANGLE, 60°; NOZZLE EXHAUST VELOCITY, 680 FT/SEC.

Figure 14. - Noise radiation comparison of the engine over the wing and under the wing models with powered lift. PNL at 500 ft.

E-7429

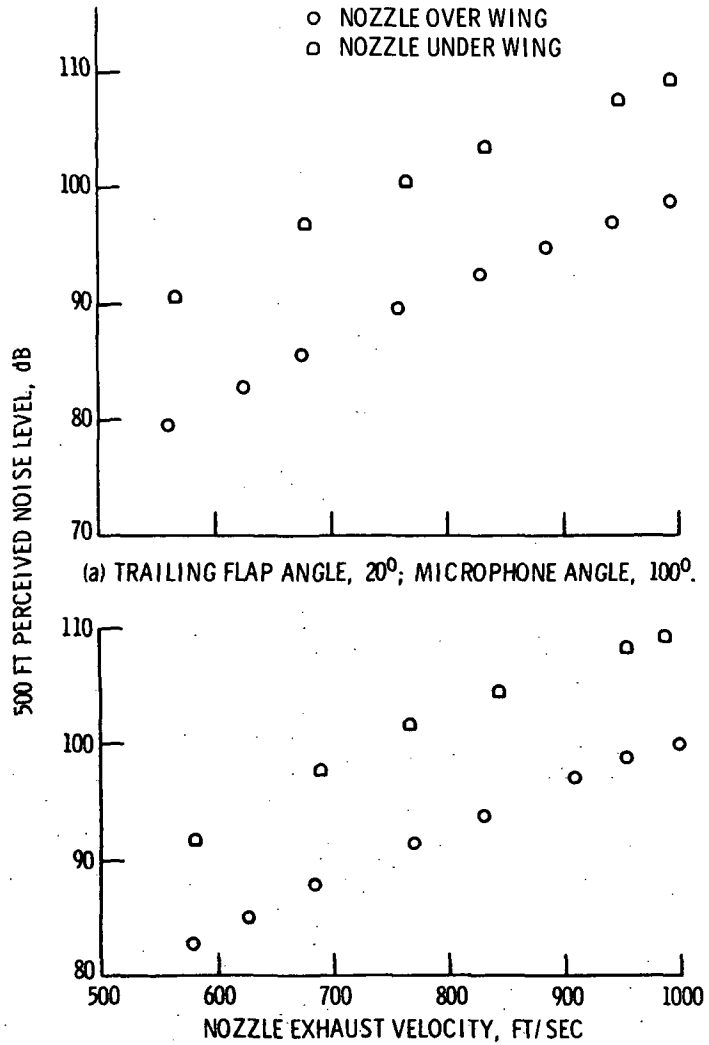

(a) TRAILING FLAP ANGLE, 20^0; MICROPHONE ANGLE, 100^0.

(b) TRAILING FLAP ANGLE, 60^0; MICROPHONE ANGLE, 80^0.

Figure 15. - Perceived noise level comparison of the engine over the wing and under the wing models with powered lift. PNL at 500 ft.

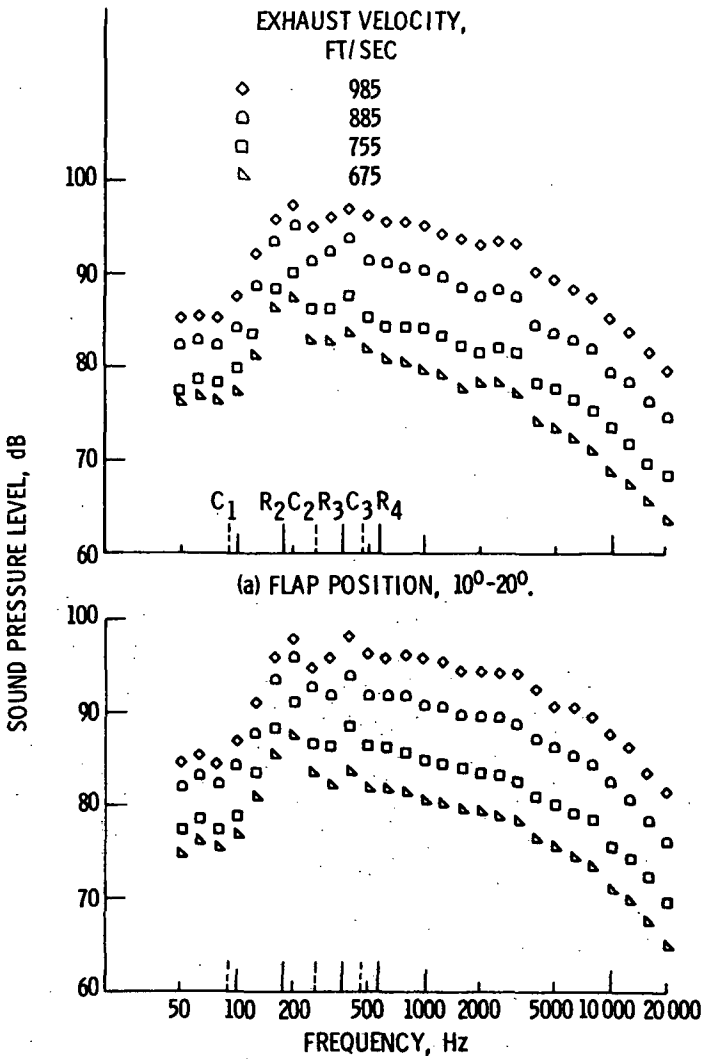

(a) FLAP POSITION, 10^0-20^0.

(b) FLAP POSITION, 30^0-60^0.

Figure 16. - EOW 1/3-octave spectra for conventional lift. Microphone at 120^0 and 50 ft.

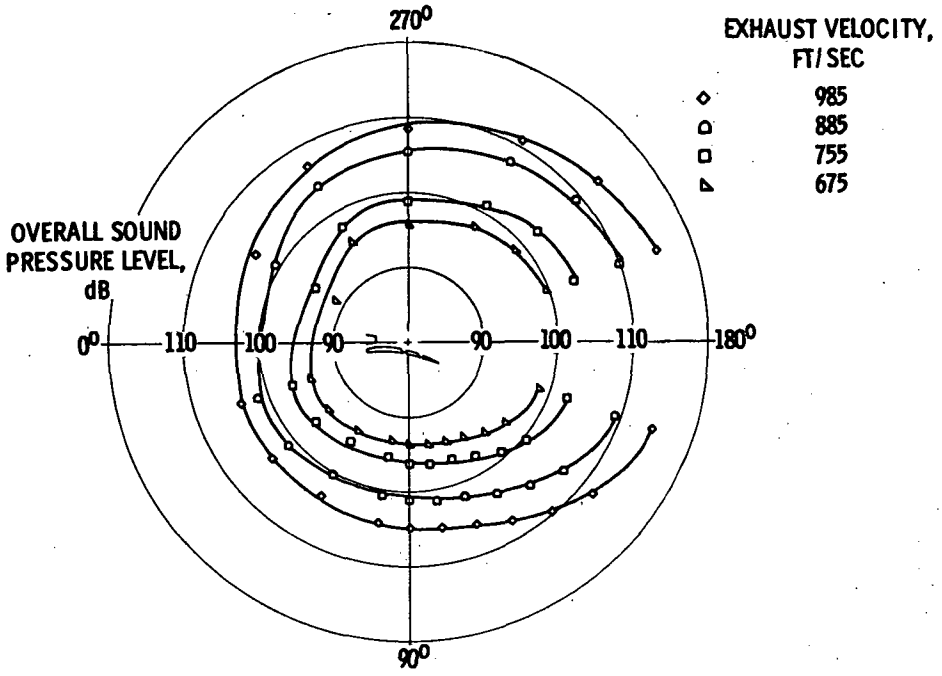

(a) FLAP POSITION, 10°-20°.

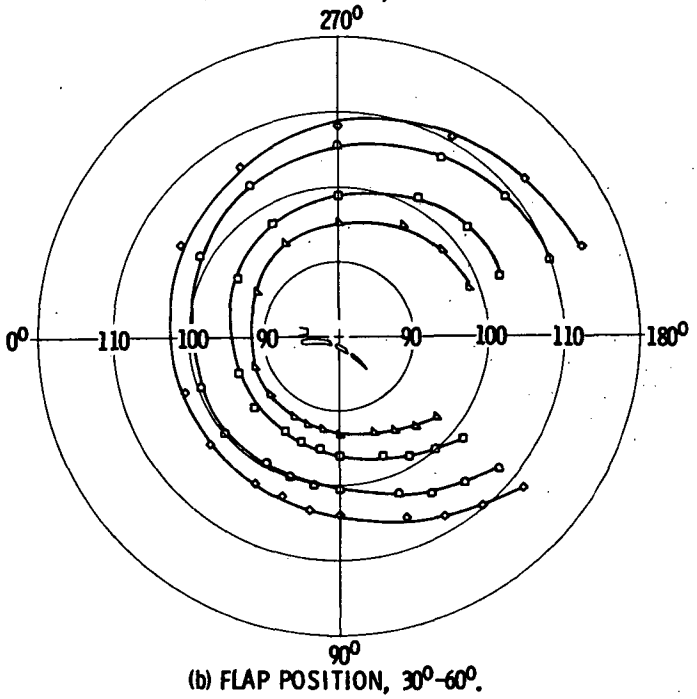

(b) FLAP POSITION, 30°-60°.

Figure 17. - EOW noise radiation patterns for conventional lift. Microphone distance, 50 ft.

E-7429

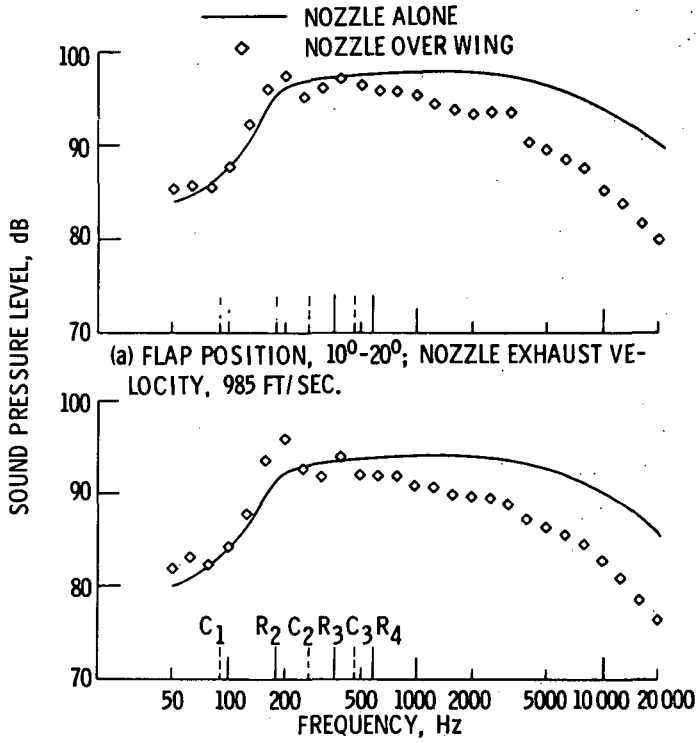

(a) FLAP POSITION, 10^0-20^0; NOZZLE EXHAUST VELOCITY, 985 FT/SEC.

(b) FLAP POSITION, 30^0-60^0; NOZZLE EXHAUST VELOCITY, 885 FT/SEC.

Figure 18. - Effect of noise shielding by the wing on the EOW configuration with conventional lift. Microphone at 120^0 and 50 ft.

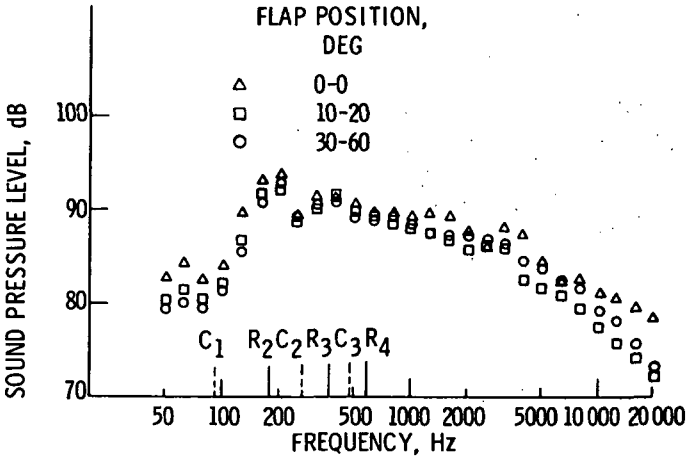

Figure 19. - Effect of flap position on the maximum below the wing noise for the EOW model with conventional lift. Microphone at 120^0 and 50 ft; nozzle exhaust velocity, 830 ft/sec.

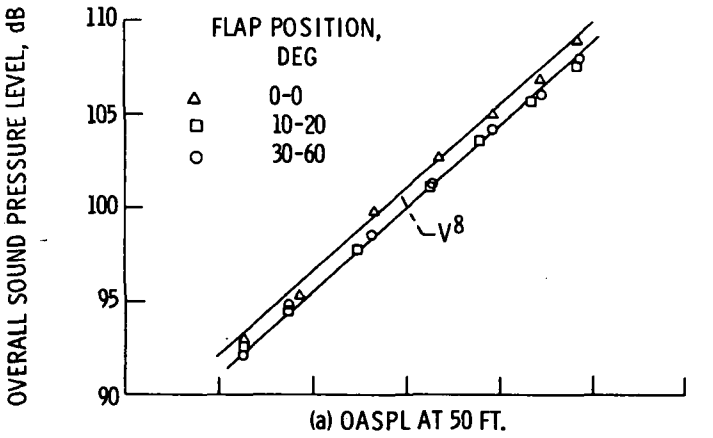

(a) OASPL AT 50 FT.

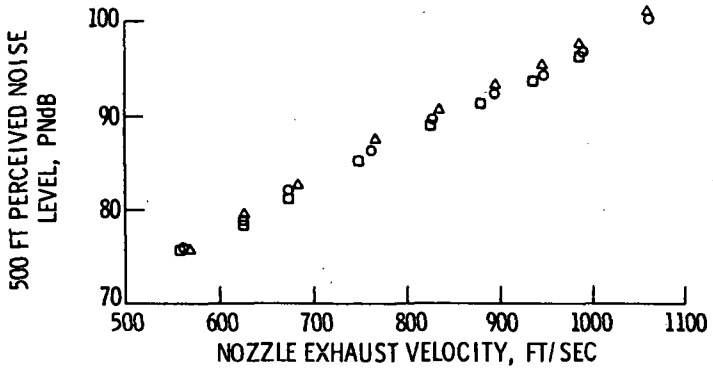

(b) PERCEIVED NOISE LEVEL AT 500 FT.

Figure 20. - Effect of exhaust velocity on the below the wing noise for the EOW model with conventional lift. Microphone angle, 120^0.

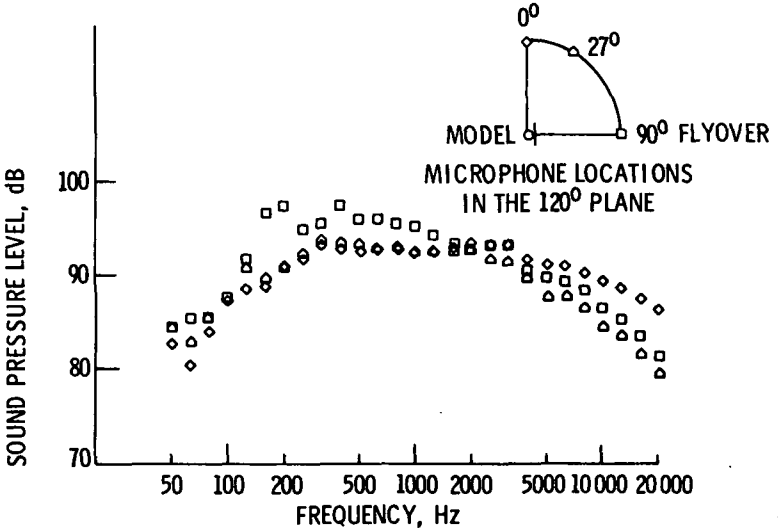

(a) 1/3-OCTAVE SPECTRA. NOZZLE EXHAUST VELOCITY, 965 FT/SEC.

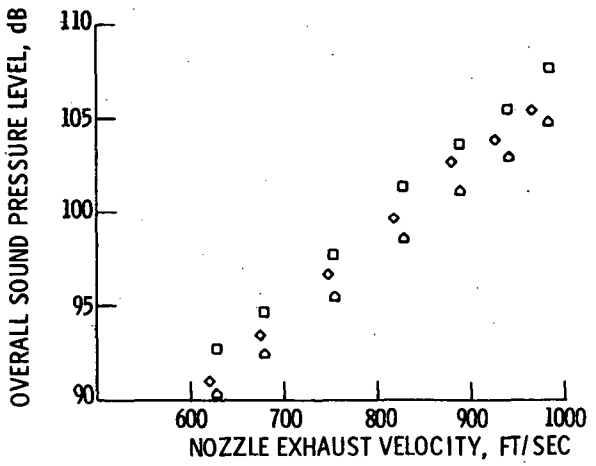

(b) OVERALL SOUND PRESSURE LEVELS.

Figure 21. - Comparison of flyover and sideline noise for the EOW model with conventional lift. Flap position, 10^0-20^0; microphones in the 120^0 plane at 50 ft.

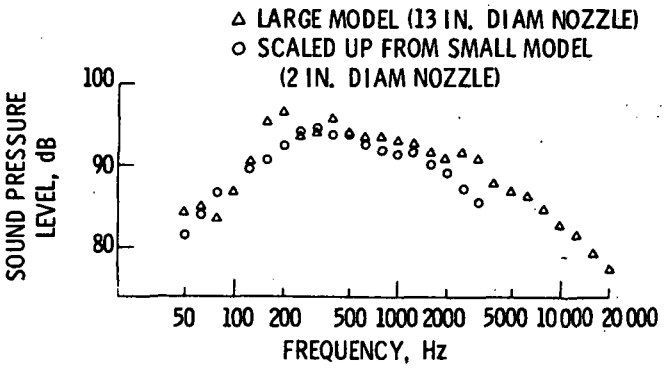

(a) 1/3-OCTAVE SPECTRA. MICROPHONE ANGLE, 120°.

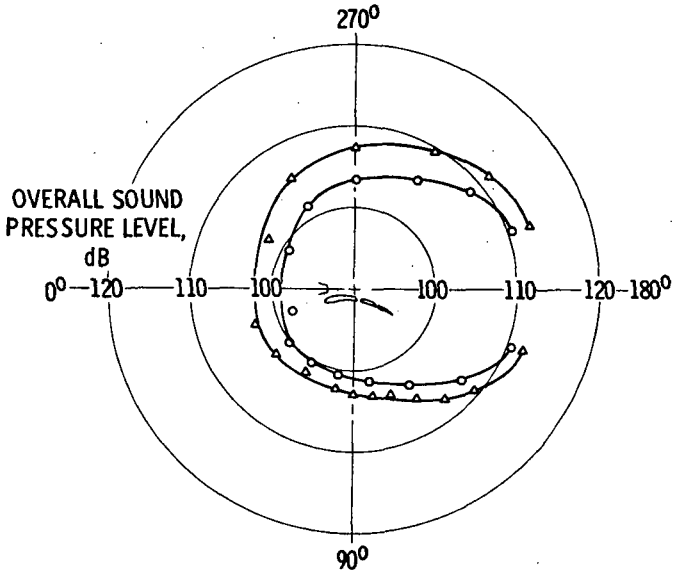

(b) NOISE RADIATION PATTERN.

Figure 22. - Comparison of large model data with scaled up small model data for the EOW configuration with conventional lift. Flap position, 10°-20°; nozzle exhaust velocity, 940 ft/sec; microphone distance, 50 ft.

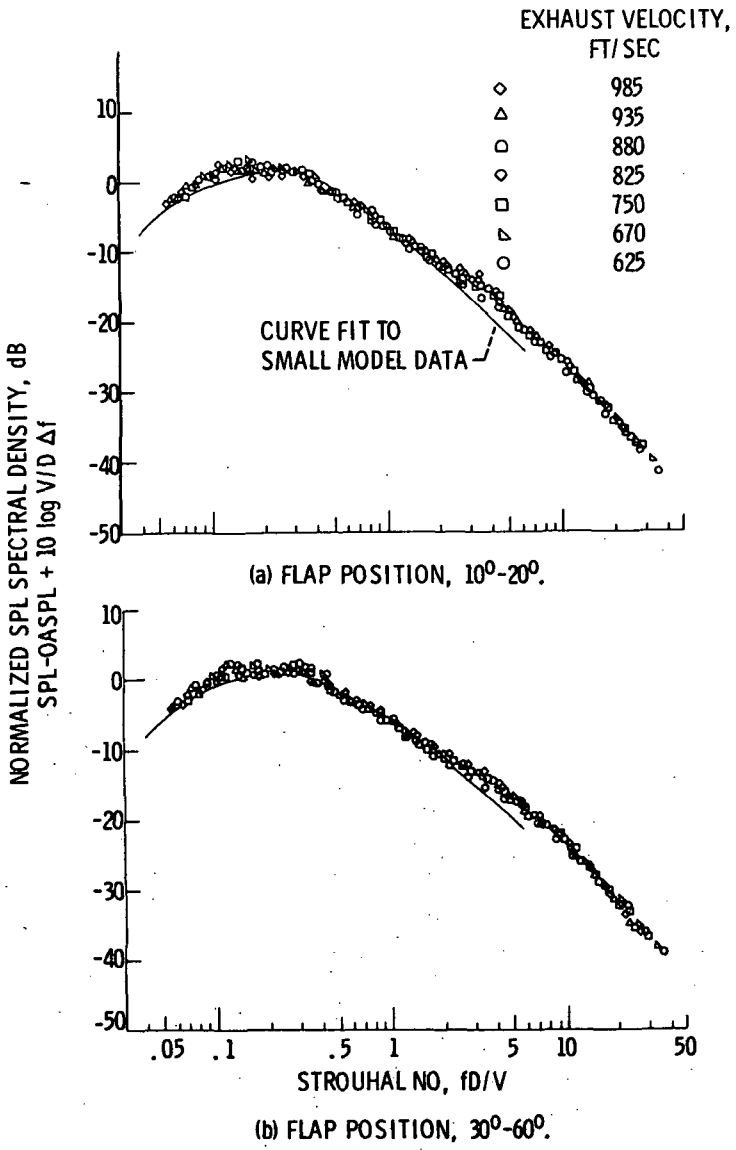

Figure 23. - A Strouhal correlation of large model data for the EOW configuration with conventional lift. Microphone angle, 120°. Corrected for ground reflections.

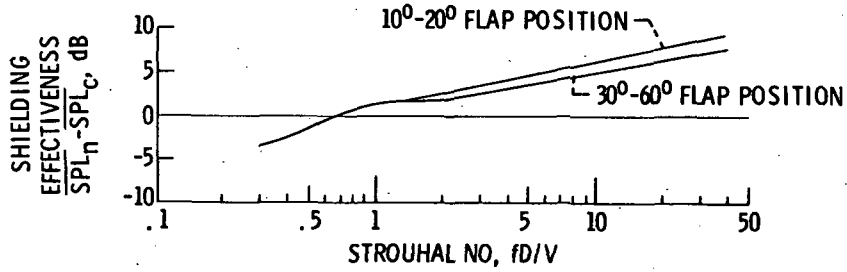

Figure 24. - Shielding effectiveness of the large model EOW configuration with conventional lift. Microphone angle, 120°. Corrected for ground reflections.

NASA-Lewis